HHS Public Access

Author manuscript

Angew Chem Int Ed Engl. Author manuscript; available in PMC 2025 July 01.

Published in final edited form as:

Angew Chem Int Ed Engl. 2024 July 01; 63(27): e202401003. doi:10.1002/anie.202401003.

Chemoselective Proteomics, Zinc Fingers, and a Zinc(II) Model for H_2S Mediated Persulfidation

Andrew T. Stoltzfus[+],
Department of Pharmaceutical Sciences, University of Maryland School of Pharmacy, 20 Penn Street, Baltimore, MD, 21201, USA

Jasper G. Ballot[+],
Department of Chemistry, Johns Hopkins University, 3400 N Charles Street, Baltimore, MD, 21218, USA

Thibaut Vignane,
Leibniz-Institut für Analytische Wissenschaften—ISAS—e.V. Dortmund, Germany, 44139

Haoju Li,
Department of Pharmaceutical Sciences, University of Maryland School of Pharmacy, 20 Penn Street, Baltimore, MD, 21201, USA

Madison M. Worth,
Department of Pharmaceutical Sciences, University of Maryland School of Pharmacy, 20 Penn Street, Baltimore, MD, 21201, USA

Ludovic Muller,
Department of Pharmaceutical Sciences, University of Maryland School of Pharmacy, 20 Penn Street, Baltimore, MD, 21201, USA

Maxime A. Siegler,
Department of Chemistry, Johns Hopkins University, 3400 N Charles Street, Baltimore, MD, 21218, USA

Maureen A. Kane,
Department of Pharmaceutical Sciences, University of Maryland School of Pharmacy, 20 Penn Street, Baltimore, MD, 21201, USA

Milos R. Filipovic[*],
Leibniz-Institut für Analytische Wissenschaften—ISAS—e.V. Dortmund, Germany, 44139

David P. Goldberg[*],
Department of Chemistry, Johns Hopkins University, 3400 N Charles Street, Baltimore, MD, 21218, USA

[*] smichel@rx.umaryland.edu, dpg@jhu.edu, milos.filipovic@isas.de.
[+]These authors contributed equally to this work.

Conflict of Interest
The authors declare no conflict of interest.

Supporting Information
The authors have cited additional references within the Supporting Information.[1,2,3c,11a,14a,15,18,22,24,26,32–35]

Sarah L. J. Michel*
Department of Pharmaceutical Sciences, University of Maryland School of Pharmacy, 20 Penn Street, Baltimore, MD, 21201, USA

Abstract

The gasotransmitter hydrogen sulfide (H_2S) is thought to be involved in the post-translational modification of cysteine residues to produce reactive persulfides. A persulfide-specific chemoselective proteomics approach with mammalian cells has identified a broad range of zinc finger (ZF) proteins as targets of persulfidation. Parallel studies with isolated ZFs show that persulfidation is mediated by zinc(II), O_2, and H_2S, and intermediates involving oxygen- and sulfur-based radicals were detected by mass spectrometry and optical spectroscopies. A small molecule zinc(II) complex exhibits analogous reactivity with H_2S and O_2, giving a persulfidated product. These data show that zinc(II) is not just a biological structural element, but also plays a critical role in mediating H_2S-dependent persulfidation. ZF persulfidation appears to be a general post-translational modification and a possible conduit for H_2S signaling. This work has broad implications for our understanding of H_2S-mediated signaling and the regulation of ZFs in cellular physiology and development.

Graphical Abstract

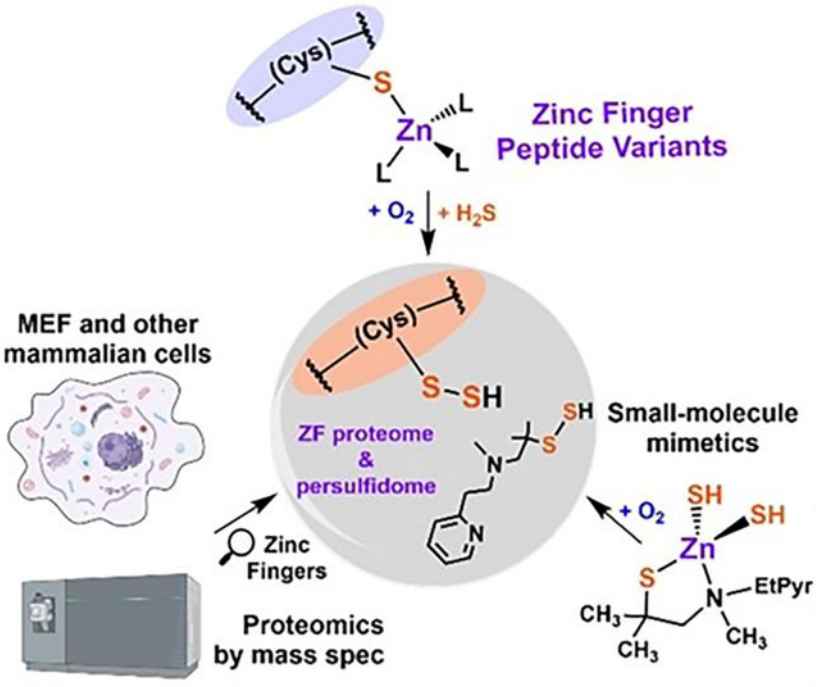

Persulfidation by H_2S is a key modification of proteins. Using persulfide specific proteomics, cysteine rich zinc finger (ZF) proteins were found to be targets of persulfidation. The reaction of H_2S with ZFs was evaluated using a series ZFs and a small molecule Zn coordination complex that mimics the ZF site. Persulfidation by H_2S occurred in an O_2 dependent manner, with the zinc acting as a conduit for electron transfer and of S–S bond formation.

Keywords

zinc finger proteins; proteomics; hydrogen sulfide; small molecules; persulfidation

Introduction

Hydrogen sulfide (H_2S) was initially identified in the 1770s as a noxious gas present in sewers.[1] It was later determined that H_2S was present on the anoxic, pre-biotic earth, about 3.8 billion years ago, and was involved in the formation of early life (see Figure S1A).[2] In the 1990s, H_2S was discovered to function as an endogenous gasotransmitter, making it the third gasotransmitter after CO and NO.[3] Many biological roles have since been ascribed to H_2S, including neuromodulation, regulation of inflammation, cardiovascular function, metabolism, transcription, and apoptosis.[4] Misregulation of H_2S is associated with inflammatory diseases such as arthritis, cardiovascular disease, and cancer.[5] Although H_2S has been proposed as a key signaling molecule in biology, a molecular level understanding of many of its mechanisms of action remains elusive.

Targets of H_2S include heme and non-heme iron proteins, reactive oxygen-, sulfur-, and nitrogen species, and cysteine residues (see Figure S1B).[1,6] The interaction of H_2S with cysteine residues, directly and indirectly, can lead to persulfidation, a post-translational modification (PTM) that involves the addition of sulfur to the Cys sulfur terminus (RSH→RSSH).[6c,7] Evidence over the last two decades suggests that persulfidation by H_2S may be a PTM involved in the regulation of many important biological processes, and developing a fundamental understanding of H_2S-mediated modifications would be of widespread significance.[1,3b,4a,6c,e,7b]

Zinc finger proteins (ZFs) were initially identified as transcription factors and were subsequently found to carry out a myriad of additional biological roles beyond transcription, including RNA regulation and protein stabilization via ZF/RNA and ZF/other protein interactions. ZFs are one of the most abundant types of cysteine-rich proteins in eukaryotes, making them ideal targets for H_2S signaling through persulfidation.[8] ZFs are comprised of domains with distinct secondary structures that include four-coordinate zinc(II) sites bound by a combination of cysteine (Cys) and histidine (His) residues.[9] Since the discovery of the first type of ZF, which contains two cysteine and two histidine residues (CCHH) that serve as ligands for zinc, at least 30 other classes of ZFs have been identified.[8c] Each class or type of ZF is delineated based upon the ligand set, fold, and function. These classes adopt a variety of secondary structures to facilitate their molecular interactions with DNA, RNA, and proteins. As such, they regulate transcription, translation, as well as protein driven regulation (e.g. ubiquitination) in multiple biological pathways. Figure 1 provides examples of four classes of ZFs. The prevailing dogma is that the Zn^{II} centers in ZFs function exclusively as structural cofactors, in keeping with their stable, d^{10} electron configurations and the absence of any biologically relevant redox chemistry.[8b,10]

There is emerging evidence of persulfidation of cysteine residues in ZFs by H_2S.[11] These data are primarily from cellular studies, and do not involve the direct assessment of the reactivity of isolated and purified ZFs with H_2S. There is a singular study of H_2S

reactivity with an isolated by ZF, reported by some of us.[11a] This work was focused on tristetraprolin (TTP) which is a CCCH type ZF protein that regulates inflammation by controlling cytokine mRNA levels in cells.[12] TTP binds to specific sequences in the 3'-UTR that are adenine and uracil rich (AU-rich), forming a protein/RNA complex that is then targeted for degradation. RNA binding by TTP requires the two CCCH domains, with Zn^{II} bound.[9] Given the role of TTP in regulating inflammation, a role also ascribed to H_2S, we sought to determine whether TTP is persulfidated by H_2S. We found evidence for persulfidation of the cysteine residues in TTP, provided that Zn^{II} was bound to TTP and the reaction with H_2S was performed under aerobic conditions. Several intermediates during persulfidation including oxygen- and sulfur-based radical species were identified. The final stage of the reaction involved disulfide bond formation, Zn^{II} ejection, and loss of TTP/RNA binding function.[11a] The data led to a proposed mechanism in which the Zn^{II} cofactor functions as both an organizational element and electron conduit, bringing the Cys target residue, H_2S, and O_2 together for electron transfer and S – S bond formation (see Scheme 1).

Our work on TTP, together with earlier ZF persulfidation studies by others[11b–h] led us to hypothesize that persulfidation of ZFs might be a general PTM, and not simply operative for a singular case of a TTP construct. We now present a chemoselective persulfide-specific proteomics study in multiple eukaryotic cells, a systematic examination of new protein constructs representing different canonical ZFs, and a novel small-molecule synthetic ZF analog.

Results and Discussion

Zinc Finger Proteins are Broadly Persulfidated in Multiple Mammalian Cell Lines

The ZF proteome in MEF was determined using deep proteome analysis. 5927 proteins were found in four biological replicates (see Table S1); of these proteins, 471 (8 %) were identified as ZFs. ZFs make up 8–10 % of eukaryotic proteomes, and these results are in line with this prediction.[8a,13] A persulfide specific cell labeling strategy that utilizes a dimedone probe to identify protein persulfides (Figure 2A)[14] revealed that 2435 proteins were endogenously persulfidated (see Table S1), of which 118 were ZFs. The ZFs were grouped based upon the ligand sets: CCCC, CCCH/CCHC and CCHH, corresponding to different types of ZFs. The most frequent ligand set found among persulfidated ZFs was CCCC (44 %), followed by CCCH/CCHC (38 %) and CCHH (18 %) (Figure 2; see also Table S2) indicating that the ZFs with more cysteine residues are persulfidated more frequently. Alternative persulfide specific proteomics methods have been applied to other cell types, and we analyzed the available data from five different human cell lines (A431, A549, U2OS, HEK293, MDA-MB-231) to determine the robustness and generality of our proteomics findings.[15] ZFs were identified in all cell lines evaluated, and a strikingly similar pattern for the frequency of persulfidation emerges: CCCC (44–61 %), CCCH/CCHC (29–38 %) and CCHH (11–18 %) (see Figure 2 and Table S2). This analysis reveals that ZF protein persulfidation occurs for a variety of ZFs in a wide range of cells from human to mouse. To our knowledge, broad persulfidation of ZFs in mammalian cells has not been documented up

to now. This has potentially far-reaching implications, suggesting that persulfidation of ZFs is a common, if not essential, mode of transport for H_2S signaling in eukaryotes.

H_2S Reactivity of Zinc Fingers with CCCC, CCCH, CCHH and CHHH Ligand Sets

The persulfide specific proteomics data revealed that a variety of ZFs can be persulfidated. ZFs can be differentiated into classes based upon their ligand set, their structure or their function. The H_2S reactivity of isolated ZF peptides with varied ligand sets (CCCC, CCCH, CCHH) was examined to determine if persulfidation of ZF sites, as seen via proteomics, occurs at the protein level. ZF domains are modular, allowing for the isolation of single peptide domains that bind Zn^{II} and fold.[9,16] ZF variants were prepared based upon TTP, which contains two CCCH ZF domains and for which a single domain (TTP-D1) has been previously isolated.[17] Three ZF variants were prepared: TTP-D1-CCCC, D1-CCHH and D1-CHHH, as well as ZF domain 2 (D2-CCCH) (for AA sequences, see Table S3). The CCCC and CCHH variants are native ZF ligand sets whereas CHHH is an abiological derivative.[9,10] All ZF peptides were isolated in the apo-form and Zn^{II} binding affinities were measured using competitive UV/Visible titrations with Co^{II} (Figure 3 and Table 1i; see also Figure S2 and Table S4).[17,18] Circular dichroism and intrinsic tyrosine fluorescence experiments showed that the ZF peptides form stable complexes with varying degrees of secondary structure (see Table 1ii; see also Figures S3, S4).

The dimedone switch method utilized for the persulfide specific proteomics screen was adapted to detect persulfidation in situ during the reaction of the ZF peptides with H_2S (see Figure S5A).[14a] $NBF^{-}Cl$ was added to each Zn-TTP peptide variant in the presence of O_2 and H_2S and the optical spectra was monitored (Figure 4A, *left*; see also Figure S5B). The NBF – Cl signal at 350 nm decreased with a concomitant increase in absorbance bands between 400 to 480 nm as the NBF labeled thiols, amines, sulfenic acids, and persulfide groups.[19] NBF labeling of persulfides forms a mixed disulfide in which one sulfur has enhanced electrophilicity, making it uniquely positioned to react with nucleophilic dimedone (the switch). Reaction with dimedone results in a decrease in the unique wavelength attributed to TTP-SS-NBF (422 nm).[14a,19,20] This switch was observed upon addition of dimedone to all Zn-TTP peptides (Figure 4A, *right*; see also Figure S5C), supporting persulfidation with a variety of ZF ligand sets. To our knowledge this is the first time that this approach has been employed to trap persulfide intermediates generated in situ, and has the potential to inform on persulfidation in other systems.[14a]

Intrinsic tyrosine fluorescence was performed on the TTP-D1- and D2-CCCH peptides to determine the effects of H_2S reactivity on ZF structure. The Zn^{II} bound peptides exhibited a fluorescence emission at 303 nm that diminished upon addition of H_2S under aerobic conditions. This suggests that persulfidation leads to protein unfolding (Figure 4B). Cryo-ESI-MS (CSI-MS), a low temperature, high-resolution mass spectrometric technique that allows for detection of native, metallated peptides and possible adducts with intermediate species, was performed on the TTP-D1-CCCH and -CCCC peptides. Adducts of peptide, superoxide ($O_2^{\bullet-}$), and dihydrogen disulfide radical anion ($H_2S_2^{\bullet-}$), were observed (Figure 4C), akin to what was previously observed for a two domain CCCH ZF construct (TTP-2D).[11a] In the case of D1-CCCH, this radical species was formed immediately upon mixing

and could be observed within the first 5 minutes of recording. Some amounts of [(TTP)($O_2^{\bullet-}$)($H_2S_2^{\bullet-}$)] were also observed when the CCCC variant was mixed with H_2S, but thiol oxidation and demetallation predominated in the same time frame suggesting that the CCCC ZF's reaction with H_2S may be faster than the CCCH ZF (see also Figure S6).

To detect the superoxide intermediates and understand the effect of ligand set, hydroethidine (HE) was utilized as a probe for superoxide anion (see Figure S7A).[21] The ZF peptides were reacted with H_2S in the presence of O_2 and HE and the change in fluorescence was monitored (emission λ = 520–680 nm; excitation λ = 466 nm). A fluorescence signal developed over time for all ZF peptides (Figure 4D; see also Figure S8) indicating the oxidation of HE by superoxide to products with greater fluorescence intensity.[22] These spectra featured peaks with λ_{max} (~595 nm) which is comparable to that of a control experiment with the xanthine/xanthine oxidase (XOD) enzyme-substrate system, which generates $O_2^{\bullet-}$; HE is oxidized by $O_2^{\bullet-}$ to form the superoxide-specific product 2-OH-E^+ (see Figure S7B).[22] Comparison of the HE signal that formed after 120 minutes between the ZF peptides revealed that the TTP-D1- and -D2-CCCH peptides, which have the native ligand set, exhibited the largest change in fluorescence signal, indicating the generation of the greatest superoxide yields (see Table S5). Additional experiments with hydroethidine and potassium superoxide (KO_2) in solvent systems of either (a) DMSO (aprotic), or (b) potassium phosphate buffer (protic) confirmed the blue-shifted fluorescence of superoxide-specific oxidation vs the red-shifted fluorescence (λ_{max}~630 nm) of non-specific HE oxidation (see Figure S7C). Taken together, the data for the ZF peptides align with the previously proposed mechanism for the persulfidation of Zn-TTP-2D, which involves reduction of oxygen to form $O_2^{\bullet-}$ (see Scheme 1).

Oxygen-dependent Persulfidation of a Synthetic $N_2S^-Zn^{II}$ Complex

The results obtained for the ZF peptides indicate that Cys persulfidation results from a Zn^{II}-mediated reaction with H_2S as the sulfur donor and O_2 as the oxidant. Such a reaction has not been previously reported for a biological zinc(II) center, and we wanted to determine if a synthetic, sulfur-ligated Zn^{II} complex with a similar coordination environment could exhibit the same reactivity. Previous work on sulfur-ligated Zn^{II} complexes have demonstrated that Zn^{II} thiolates are activated towards polysulfide formation, but the reactivity of Zn^{II} thiolates with H_2S and O_2 has yet to be investigated.[23] The structurally well-defined Zn-(PATH)Br (**1**) (PATH= 2-methyl-1-[methyl-(2-pyridin-2-yl-ethyl)amino]propane-2-thiol) [24] provides a Zn^{II} center with a biomimetic N_2S(alkylthiolate) coordination environment and a single thiolato donor, simplifying the analysis for persulfidated product. Complex **1** reacts with SH^- salts to give the new Zn(PATH)(SH) (**2**) as colorless crystals suitable for X-ray structure determination (Figure 5C; see also Table S6). The crystal structure reveals a pseudotetrahedral Zn^{II} complex in which the bromide ligand of **1** has been replaced by a terminal hydrosulfide group. To our knowledge, **2** is the first example of a Zn^{II} complex with both a terminal SH^- and a thiolato group in the first coordination sphere. The structure of **2** is also notable in that little steric protection of the SH^- group is provided to prevent Zn S(H)-Zn bridged structures, as opposed to the few other isolable, mononuclear Zn^{II}(SH) complexes.[1,25] The ^1H nuclear magnetic resonance (NMR) spectrum of **2** versus starting material **1** (see Figure S9) shows significant differences, including two new singlets at 1.47

and 1.25 ppm, which are assigned to the diastereotopic, geminal methyl substituents. A new upfield resonance at −1.9 ppm can also be seen for **2**, corresponding to the terminal SH^- group.[25b] The ^1H NMR data confirm that the crystal structure of **2** remains intact in solution.

Complex **2** was surprisingly inert to O_2, but we hypothesized that addition of excess SH^- might lead to enhanced reactivity, and possibly persulfidation. This idea was based on the proposed mechanism for the persulfidation of TTP, which includes a $Zn^{II}–H_2S_2^{\bullet-}$ intermediate as shown in (see Scheme 1). Addition of 1 equivalent of $[(PPh_3)_2N][SH]$ to **2** under anaerobic conditions in CD_3CN leads to a ^1H NMR spectrum consistent with displacement of the pyridine arm by SH^-. Analysis of the reaction mixture by FTIR spectroscopy reveals that the vibrational mode for the coordinated pyridyl group (1607 cm^{-1}) shifts to that seen for the free ligand (1587 cm^{-1})(see Figure S10).[26] Together the NMR and IR data indicate that the pyridyl donor has been displaced by a second equivalent of SH^-, leading to $[Zn\text{-}(PATH)(SH)_2]^-$ (**3**) (Figure 5A; see also Figure S11). This assignment was confirmed by high-resolution ESI-MS (negative ion mode, see Figure S12). This complex is reminiscent of the CCCH-ZF shown in Figure 1, with 3 anionic sulfur ligands and one neutral nitrogen donor.

Unlike complex **2**, the bis(sulfhydryl)-zinc(II) species **3** reacts with O_2, as seen by a gradual color change from colorless to yellow. The addition of an extra equivalent of SH^- to **3** helps push the equilibrium toward complete formation of the bis(SH)-ligated species **3**, and addition of excess O_2 gas under these conditions leads to persulfidation of the PATH ligand (Figure 5A). The persulfidated ligand was identified following demetallation via an acid/base protocol, which resulted in a mixture of persulfidated product together with some free PATH ligand, as seen by ^1H NMR spectroscopy (see Figure S13). The identity of the persulfidated product was confirmed by high-resolution EI-MS ($[M^+]$ = 256.1071 m/z, calculated 256.1067 m/z; see Figure S14), and integration by ^1H NMR against an internal standard gives a persulfidated yield of 11.8 0.2 % (see Figure S15). This relatively modest yield is likely a result of persulfide degradation during work-up; persulfides are well known to be unstable and their isolation is challenging.[1–2,27] Several control reactions were carried out to determine the requirements for persulfidation, as shown in Figure 5B. The mono-sulfhydryl species **2** is unreactive toward O_2 (see Figure S16) and no persulfidation occurs for the bis(sulfhydryl) species **3** in the absence of O_2 or excess SH^- (see Figure S17). Free PATH ligand does not undergo persulfidation, giving instead unidentified products in the presence of excess O_2 and SH^- (see Figure S18). Taken together, these data show that both zinc(II) and O_2 are required for the SH^- mediated persulfidation of the alkylthiolate donor in PATH. This work provides a synthetic example of persulfidation with a Zn^{II}-SR complex, SH^- and O_2.

Conclusion

The modification of cysteine residues to persulfides by H_2S is emerging as an important PTM thought to be connected to signaling by H_2S. This PTM is widely observed, for example, it is estimated that 30 % of proteins are persulfidated under resting conditions.[6e,28] However, the types of proteins that are persulfidated are not well defined,

underscoring the importance of identifying proteins that are persulfidated by H_2S. The persulfide specific proteomics data presented here identified cysteine rich ZFs as a type of protein that is widely persulfidated in mammalian cells. Persulfidation occurred for different classes of ZFs (i.e. with different ligand sets and different functions), suggesting that ZF persulfidation is broad. This finding challenges the long-held dogma that ZFs use the Zn^{II} center for solely structural purposes. Our investigation of the reactivity of a series of isolated ZF peptides with varied ligand sets as well as with a small synthetic, sulfur-ligated zinc(II) complex with a similar coordination environment as the ZFs, offered further evidence for reactivity at the Zn^{II} center, as well as mechanistic insight. The reaction of ZFs requires O_2, and the data support a mechanism whereby Zn^{II} serves as a conduit for electron transfer between O_2 and HS^-, similar to those proposed for iron and manganese dioxygenases[29] and models of Zn^{II} superoxide dismutase.[30]

Persulfidation of cysteine residues (RSH→RSSH) is emerging as an important modification for posttranslational regulation of protein function.[1,7c] In addition to the enzyme activation and inactivation, persulfidation also has a protective role, serving as the evolutionarily conserved protective loop for protection of thiols from overoxidation.[14a] This is best evidenced in protection against oxidative stress in aging.[14a,31]

The finding that a variety of ZFs are persulfidated, including those with different ligand sets (e.g. CCCC versus CCCH) and functions (e.g. transcription versus RNA regulation), brings up the question of the biological significance of ZF persulfidation. To holistically answer this question, detailed biological studies of each ZF identified as persulfidated are needed; however, there are already a few published studies on these effects, from which we can draw some preliminary conclusions. One of the studies is work by our laboratory, on TTP (CCCH type), in which we reported that persulfidation increases TNFα RNA levels.[11a] TTP regulates cytokine mRNAs, including TNFα, and this finding supports a model by which H_2S modulates mRNA regulation via TTP. Another study focused on the androgen receptor (AR) which is a CCCC type ZF that functions as a transcription factor; here, ZF persulfidation was linked to a reduction of the expression of AR target genes, indicating that H_2S downregulates transcription for this specific protein.[11c] Another example is work on Sirtuin, a protein that regulates deacetylation of histones and includes a singular CCCC type ZF domain that provides a structural element to indirectly regulate deacetylase activity. Here, persulfidation of the ZF promoted deacetylase activity.[11e,f] Additional studies include work on Parkin, a protein that has E3 uibiquitin ligase activity and contains a RING type (CCCH–CCCC), that revealed that persulfidation is connected to increased ligase activity[11b] and work on SP1, a CCHH ZF that regulates transcription, that showed that persulfidation leads to enhanced transcription of VEGF-1 by SP1.[11d] These collective findings reveal that persulfidation can enhance or decrease specific ZF protein activity related to transcription, translation and enzymatic activity (indirectly via a structural role of the ZF), and suggest that as additional studies focused on the biological significance are reported, a variety of effects on function will be discovered.

A major role for ZFs in biology is to regulate transcription and translation, and a myriad of biological processes rely on this ZF activity. This regulation requires that Zn^{II} is bound to the ZF such that the protein is folded and can directly interact with the DNA or RNA

sequence associated with the transcriptional or translational event. The data presented here show that Zn^{II} centers react with H_2S and O_2 to give persulfidated ZFs and metal ion release, suggesting an intriguing new mechanism for transcriptional/translational control.

Supplementary Material

Refer to Web version on PubMed Central for supplementary material.

Acknowledgements

We thank Prof. Dr. Ivana Ivanovic-Burmazovic, Ludwig-Maximilians-Universität München, Munich, Germany, for use of the ultra-high-resolution cryo-spray-ionization mass spectrometer. S.L.J.M. is grateful to the NIH for funding (R01GM139854). D.P.G. is grateful to the NIH for funding (R35GM149233). Figures were prepared with the following software: Biorender, Kaleidagraph (Synergy software), and ChemDraw (PerkinElmer).

Data Availability Statement

Additional data that support the findings of this article are available in the supplementary material online. CCDC reference 2254803 contains the complete crystallographic data for **2** used in this study. These data are freely accessible at https://www.ccdc.cam.ac.uk/structures/. All mass spectrometric proteomics data, protein identification, and quantification results have been deposited with the ProteomeXchange Consortium via the PRIDE partner repository with the dataset identifier PXD041310 and 10.6019/PXD041310. These data are freely accessible at https://www.ebi.ac.uk/pride/.

References

[1]. Filipovic MR, Zivanovic J, Alvarez B, Banerjee R, Chem. Rev. 2018, 118, 1253–1337. [PubMed: 29112440]

[2]. Olson KR, Free Radical Biol. Med. 2019, 140, 74–83. [PubMed: 30703482]

[3]. a)Hosoki R, Matsuki N, Kimura H, Biochem. Biophys. Res. Commun. 1997, 237, 527–531; [PubMed: 9299397] b)Paul BD, Snyder SH, Nat. Rev. Mol. Cell Biol. 2012, 13, 499–507; [PubMed: 22781905] c)Hartle MD, Pluth MD, Chem. Soc. Rev. 2016, 45, 6108. [PubMed: 27167579]

[4]. a)He B, Zhang Z, Huang Z, Duan X, Wang Y, Cao J, Li L, He K, Nice EC, He W, Gao W, Shen Z, Biochem. Pharmacol. 2023, 209, 115444; [PubMed: 36736962] b)Sbodio JI, Snyder SH, Paul BD, Br. J. Pharmacol. 2019, 176, 583–593. [PubMed: 30007014]

[5]. a)Donnarumma E, Trivedi RK, Lefer DJ, Compr. Physiol. 2017, 7, 583–602; [PubMed: 28333381] b)Kimura H, Antioxid. Redox Signaling 2015, 22, 362–376.

[6]. a)Basudhar D, Ridnour LA, Cheng R, Kesarwala AH, Heinecke J, Wink DA, Coord. Chem. Rev. 2016, 306, 708–723; [PubMed: 26688591] b)Kabil O, Banerjee R, Antioxid. Redox Signaling 2014, 20, 770–782;c)Fukuto JM, Ignarro LJ, Nagy P, Wink DA, Kevil CG, Feelisch M, Cortese-Krott MM, Bianco CL, Kumagai Y, Hobbs AJ, Lin J, Ida T, Akaike T, FEBS Lett. 2018, 592, 2140–2152; [PubMed: 29754415] d)Vitvitsky V, Miljkovic JL, Bostelaar T, Adhikari B, Yadav PK, Steiger AK, Torregrossa R, Pluth MD, Whiteman M, Banerjee R, Filipovic MR, ACS Chem. Biol. 2018, 13, 2300–2307; [PubMed: 29966080] e)Doka E, Ida T, Dagnell M, Abiko Y, Luong NC, Balog N, Takata T, Espinosa B, Nishimura A, Cheng Q, Funato Y, Miki H, Fukuto JM, Prigge JR, Schmidt EE, Arner ESJ, Kumagai Y, Akaike T, Nagy P, Sci. Adv. 2020, 6, eaax8358. [PubMed: 31911946]

[7]. a)Cuevasanta E, Lange M, Bonanata J, Coitino EL, Ferrer-Sueta G, Filipovic MR, Alvarez B, J. Biol. Chem. 2015, 290, 26866–26880; [PubMed: 26269587] b)Paul BD, Snyder SH, Trends

Biochem. Sci. 2015, 40, 687–700; [PubMed: 26439534] c)Vignane T, Filipovic MR, Antioxid. Redox Signaling 2023, 39, 19–39.

[8]. a)Andreini C, Banci L, Bertini I, Rosato A, Proteome Res J. 2006, 5, 196–201;b)Andreini C, Banci L, Bertini I, Rosato A, Proteome Res J. 2006, 5, 3173–3178;c)Ok K, Filipovic MR, Michel SLJ, Eur. J. Inorg. Chem. 2021, 2021, 3795–3805; [PubMed: 34867080] d)Wiedemann C, Kumar A, Lang A, Ohlenschlager O, Front. Chem. 2020, 8, 280. [PubMed: 32391319]

[9]. Lee SJ, Michel SL, Acc. Chem. Res. 2014, 47, 2643–2650. [PubMed: 25098749]

[10]. Pace NJ, Weerapana E, Biomol. Eng. 2014, 4, 419–434.

[11]. a)Lange M, Ok K, Shimberg GD, Bursac B, Markó L, Ivanović-Burmazović I, Michel SLJ, Filipovic MR, Angew. Chem. Int. Ed. 2019, 131, 8081–8085;b)Vandiver MS, Paul BD, Xu R, Karuppagounder S, Rao F, Snowman AM, Ko HS, Lee YI, Dawson VL, Dawson TM, Sen N, Snyder SH, Nat. Commun. 2013, 1626; [PubMed: 23535647] c)Zhao K, Li S, Wu L, Lai C, Yang G, J. Biol. Chem. 2014, 289, 20824–20835; [PubMed: 24942741] d)Saha S, Chakraborty PK, Xiong X, Dwivedi SK, Mustafi SB, Leigh NR, Ramchandran R, Mukherjee P, Bhattacharya R, FASEB J. 2016, 30, 441–56; [PubMed: 26405298] e)Yuan Y, Zhu L, Li L, Liu J, Chen Y, Cheng J, Peng T, Lu Y, Antioxid. Redox Signaling 2019 31, 1302–1319;f)Du C, Lin X, Xu W, Zheng F, Cai J, Yang J, Cui Q, Tang C, Cai J, Xu G, Geng B, Antioxid. Redox Signaling 2019, 30, 184–197;g)Dey A, Prabhudesai S, Zhang Y, Rao G, Thirugnanam K, Hossen MN, Dwivedi SKD, Ramchandran R, Mukherjee P, Bhattacharya R, Sci. Adv. 2020, 6;h)Liu D, Song H, Li Y, Huang R, Liu H, Tang K, Jiao N, Liu J, Antioxidants 2023, 12. [PubMed: 38275630]

[12]. a)Tiedje C, Diaz-Munoz MD, Trulley P, Ahlfors H, Laass K, Blackshear PJ, Turner M, Gaestel M, Nucleic Acids Res. 2016, 44, 7418–7440; [PubMed: 27220464] b)Alkallas R, Fish L, Goodarzi H, Najafabadi HS, Nat. Commun. 2017, 8, 909. [PubMed: 29030541]

[13]. Bertini I, Decaria L, Rosato A, J. Biol. Inorg. Chem. 2010, 15, 1071–1078. [PubMed: 20443034]

[14]. a)Zivanovic J, Kouroussis E, Kohl JB, Adhikari B, Bursac B, Schott-Roux S, Petrovic D, Miljkovic JL, Thomas-Lopez D, Jung Y, Miler M, Mitchell S, Milosevic V, Gomes JE, Benhar M, Gonzalez-Zorn B, Ivanovic-Burmazovic I, Torregrossa R, Mitchell JR, Whiteman M, Schwarz G, Snyder SH, Paul BD, Carroll KS, Filipovic MR, Cell Metab. 2019, 30, 1152–1170 e1113; [PubMed: 31735592] b)Aroca A, Jurado-Flores A, Filipovic MR, Gotor C, Romero LC, Methods Enzymol. 2022, 676, 385–402; [PubMed: 36280359] c)Pedre B, Talwar D, Barayeu U, Schilling D, Luzarowski M, Sokolowski M, Glatt S, Dick TP, Nat. Chem. Biol. 2023, 19, 507–517; [PubMed: 36732619] d)Garcia-Calderon M, Vignane T, Filipovic MR, Ruiz MT, Romero LC, Marquez AJ, Gotor C, Aroca A, New Phytol. 2023, 238, 1431–1445; [PubMed: 36840421] e)Bibli SI, Hu J, Looso M, Weigert A, Ratiu C, Wittig J, Drekolia MK, Tombor L, Randriamboavonjy V, Leisegang MS, Goymann P, Delgado Lagos F, Fisslthaler B, Zukunft S, Kyselova A, Justo AFO, Heidler J, Tsilimigras D, Brandes RP, Dimmeler S, Papapetropoulos A, Knapp S, Offermanns S, Wittig I, Nishimura SL, Sigala F, Fleming I, Circulation 2021, 143, 935–948. [PubMed: 33307764]

[15]. Fu L, Liu K, He J, Tian C, Yu X, Yang J, Antioxid. Redox Signaling 2020, 33, 1061–1076.

[16]. Negi S, Imanishi M, Hamori M, Kawahara-Nakagawa Y, Nomura W, Kishi K, Shibata N, Sugiura Y, J. Biol. Inorg. Chem. 2023, 28, 249–261. [PubMed: 36749405]

[17]. Michel SL, Guerrerio AL, Berg JM, Biochemistry 2003, 42, 4626–4630. [PubMed: 12705825]

[18]. Stoltzfus AT, Campbell CJ, Worth MM, Hom K, Stemmler TL, Michel SLJ, J. Biol. Inorg. Chem. 2023, 28, 85–100. [PubMed: 36478265]

[19]. Ellis HR, Poole LB, Biochemistry 1997, 36, 15013–15018. [PubMed: 9398227]

[20]. a)Ghosh PB, Whitehouse MW, Biochem. J. 1968, 108, 155–156; [PubMed: 5657448] b)Gupta V, Carroll KS, Biochim. Biophys. Acta. 2014, 1840, 847–875. [PubMed: 23748139]

[21]. Hardy M, Zielonka J, Karoui H, Sikora A, Michalski R, Podsiadly R, Lopez M, Vasquez-Vivar J, Kalyanaraman B, Ouari O, Antioxid. Redox Signaling 2018, 28, 1416–1432.

[22]. Zhao H, Kalivendi S, Zhang H, Joseph J, Nithipatikom K, Vásquez-Vivar J, Kalyanaraman B, Free Radical Biol. Med. 2003, 34, 1359–1368. [PubMed: 12757846]

[23]. a)Ballesteros MI, Tsui EY, Inorg. Chem. 2019, 58, 10501–10507; [PubMed: 31247870] b)Seo WT, Ballesteros MI, Tsui EY, J. Am. Chem. Soc. 2022, 144, 20630–20640. [PubMed: 36326496]

[24]. Chang S, Karambelkar VV, diTargiani RC, Goldberg DP, Inorg. Chem. 2001, 40, 194–195. [PubMed: 11170522]

[25]. a)Hartle MD, Delgado M, Gilbertson JD, Pluth MD, Chem. Commun. 2016, 52, 7680–7682;

b). Melnick JG, Docrat A, Parkin G, Chem. Commun. 2004, 2870–2871.

[26]. Brand U, Vahrenkamp H, Inorg. Chim. Acta 2000, 308, 97–102.

[27]. Hankins RA, Suarez SI, Kalk MA, Green NM, Harty MN, Lukesh JC 3rd, Angew. Chem. Int. Ed. 2020, 59, 22238–22245.

[28]. Sen N, Paul BD, Gadalla MM, Mustafa AK, Sen T, Xu R, Kim S, Snyder SH, Mol. Cell 2012, 45, 13–24. [PubMed: 22244329]

[29]. Emerson JP, Kovaleva EG, Farquhar ER, Lipscomb JD, Que L Jr., Proc. Natl. Acad. Sci. USA 2008, 105, 7347–7352. [PubMed: 18492808]

[30]. Ward MB, Scheitler A, Yu M, Senft L, Zillmann AS, Gorden JD, Schwartz DD, Ivanovic-Burmazovic I, Goldsmith CR, Nat. Chem. 2018, 10, 1207–1212. [PubMed: 30275506]

[31]. Dey A, Pramanik PK, Dwivedi SKD, Neizer-Ashun F, Kiss T, Ganguly A, Rice H, Mukherjee P, Xu C, Ahmad M, Csiszar A, Bhattacharya R, Redox Biol. 2023, 68, 102958. [PubMed: 37948927]

[32]. Gingerich RGW, Angelici RJ, J. Am. Chem. Soc. 1979, 101, 5604–5608.

[33]. a)Bogdándi V, Ida T, Sutton TR, Bianco C, Ditrói T, Koster G, Henthorn HA, Minnion M, Toscano JP, van der Vliet A, Pluth MD, Feelisch M, Fukuto JM, Akaike T, Nagy P, Br. J. Pharmacol. 2019, 176, 646–670; [PubMed: 29909607] b)Bailey TS, Henthorn HA, Pluth MD, Inorg MD, Chem. 2016, 55, 12618–12625.

[34]. a)Sherbow TJ, Zakharov LN, Johnson DW, Pluth MD, Inorg. Chem. 2020, 59, 15574–15578; [PubMed: 33045168] b)Li K, Zakharov LN, Pluth MD, J. Am. Chem. Soc. 2023, 145, 13435–13443. [PubMed: 37294127]

[35]. Sheldrick GM, Acta Crystallogr. 2015, 71, 3–8.

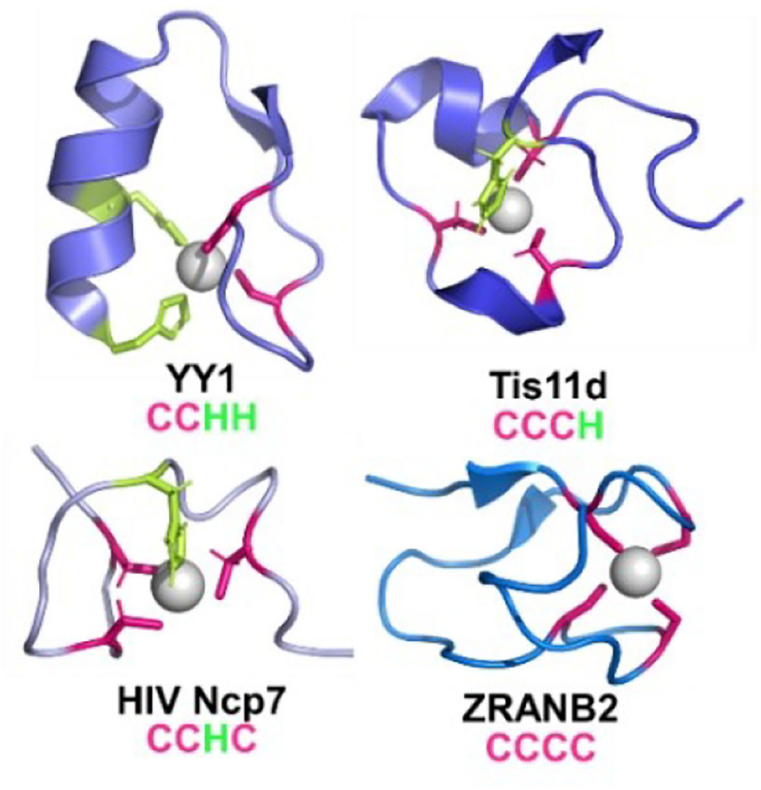

Figure 1.
Structures of four different ZF domains/ligand sets; Cys colored pink and His green (made in PyMol, PDB: YY1: 1UBD; Tis11d: 1RGO; HIV Ncp7: 2L44; ZRANB2: 3G9Y).

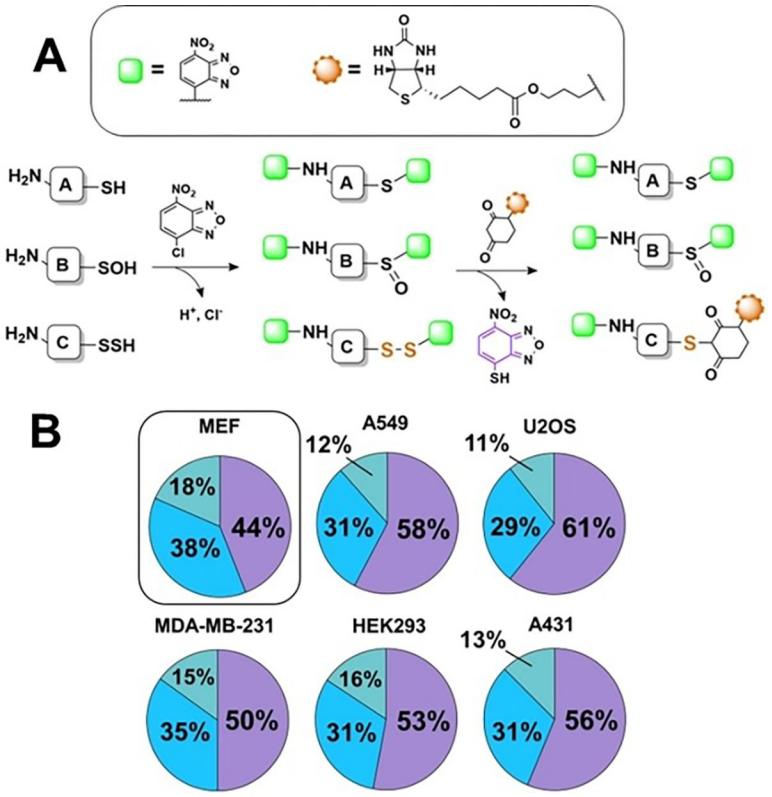

Figure 2.

A) Reaction Scheme of dimedone-switch labeling of cellular persulfides for proteomics analysis. B) Pie charts representing the distribution of persulfidated ZFs in different cell types, sorted by ZF ligand set: CCCC (purple), CCCH or CCHC (blue), and CCHH (cyan).

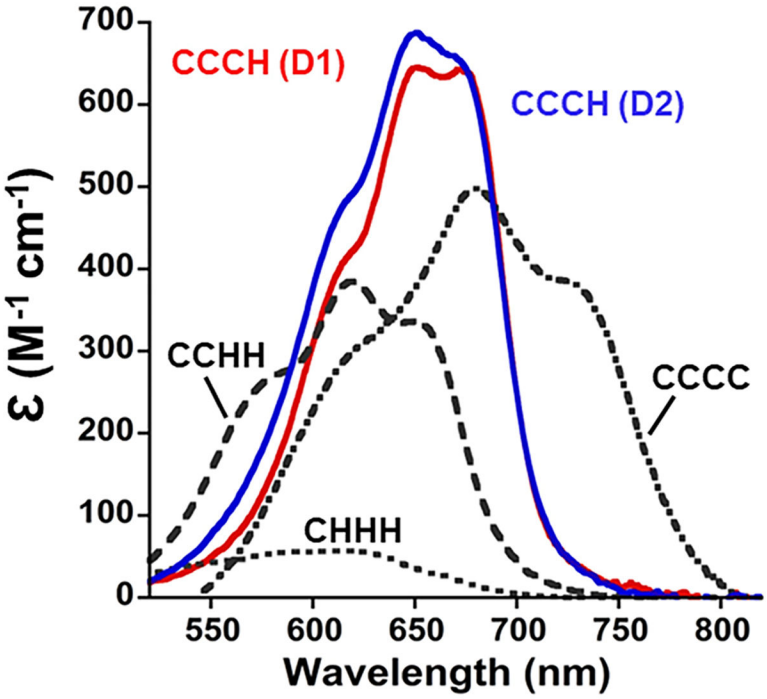

Figure 3.
UV/Visible spectra from 520 to 820 nm of the apo-ZF peptides upon addition of 1 equivalent of $CoCl_2$ (50 mM HEPES, pH 7.5).

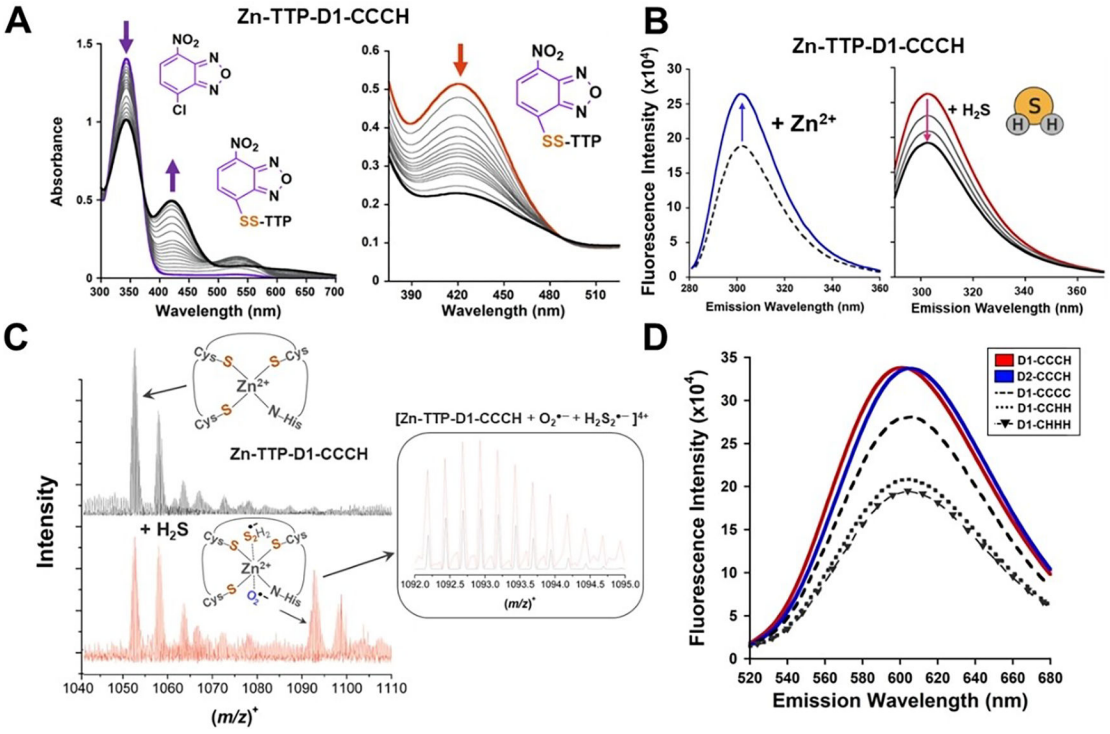

Figure 4.

A) UV/Visible spectra of Zn-TTP-D1-CCCH reacted with Na_2S in 100 mM HEPES, pH 7.5. *Left:* plot of spectrum between 300–700 nm after exposure to O_2 and addition of $NBF^{-}Cl$ (purple), followed by the spectra obtained every 30s (grey traces) until no further spectral changes observed (black). *Right:* plot of spectrum between 375–525 nm following addition of dimedone to the same reaction mixture (red), followed by the spectra obtained every 30s (grey traces) until no further change observed (black). B) Plot of the change in the intrinsic tyrosine fluorescence spectrum as apo-TTP-D1-CCCH is bound with Zn^{II} (dashed black to solid blue trace, left) and reacted aerobically with H_2S over 30 minutes (red to black trace, right). C) CSI-MS spectra of the z= 4 + species of Zn-TTP-D1-CCCH (40 μM) in 20 mM NH_4HCO_3 (pH 7.4), before (upper panel) and after (middle panel) addition of 400 μM Na_2S under aerobic conditions. *Inset:* simulated (blue) and experimental (red) spectra overlaid for the intermediate species observed at 1092 *m/z.* D) Fluorescence emission spectra of oxidized hydroethidine after the reaction of ZF peptides with H_2S (aerobic, t= 120 minutes, 50 mM sodium phosphate, pH 7.5).

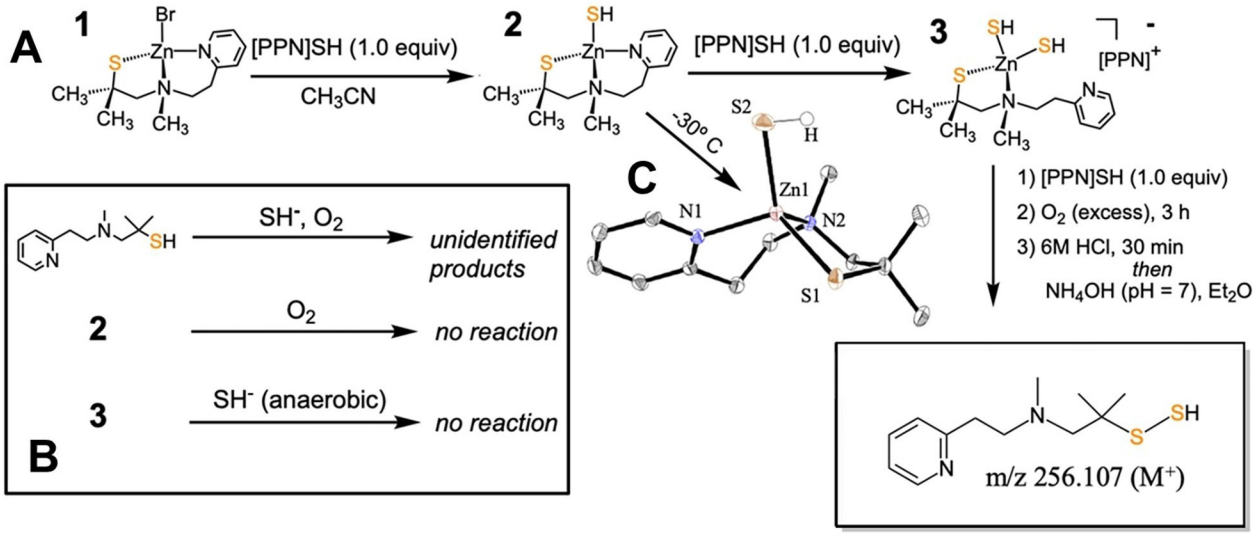

Figure 5.

A) Synthesis of complexes 2 and 3, and persulfidation reaction with O_2. B) Control reactions between free ligand PATH, $[(PPh_3)_2N][SH]$ and O_2 (top), 2 and O_2 (middle), 3 and $[(PPh_3)_2N][SH]$ under anaerobic conditions (bottom), showing no formation of persulfide product in each case. C) Displacement ellipsoid plot (50 % probability level) of 2 at 110(2) K. Hydrogen atoms (except for S–H) are omitted for clarity.

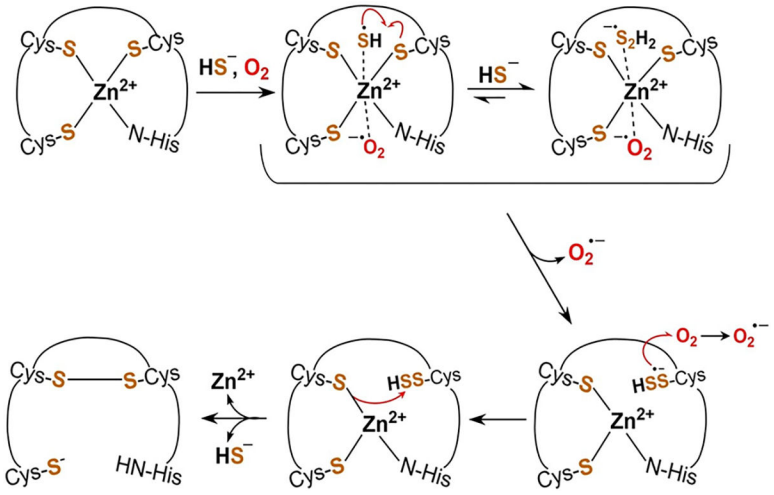

Scheme 1.

Proposed mechanism for the persulfidation of zinc finger domains by H_2S in the presence of O_2. The initial HS^- coordination to the Zn^{II} site, which acts as a conduit for the anionic species present, facilities reduction of O_2 and activation of HS^- to the thiyl radical species ($HS^{\bullet}$). This species could react with additional HS^- present or form a perthiyl radical ($HSS^{\bullet-}$) with a proximal Cys residue. Further reaction with ambient oxygen can form the persulfide group (SSH), and depending upon the current oxidative environment, the complete oxidation to a disulfide bond occurs.

Table 1:

(i) Upper limit Zn^{II} binding affinities (K_d) for TTP peptides obtained from Co/Zn competitive titrations and (ii) observed change in fluorescence, as fold increase, for direct titrations of TTP variants with Zn^{II}.

TTP Peptide	(i) Zn^{II} K_d (M) [a]	(ii) Fluorescence Fold Increase [a]
D2-CCCH	$1.4\times10^{-9}\pm2.0\times10^{-10}$	1.30±0.02
D1-CCCH	$2.1\times10^{-9}\pm2.8\times10^{-10}$	1.37±0.02
D1-CCCC	$2.7\times10^{-9}\pm5.0\times10^{-10}$	1.11±0.01
D1-CCHH	$1.6\times10^{-10}\pm1.7\times10^{-11}$	1.14±0.01
D1-CHHH	$3.1\times10^{-7}\pm1.5\times10^{-7}$	1.01±0.01

[a] Numbers following the ± are S.E.M. from replicate experiments (N = 3)